# Phase diagram of magnetic domain walls in spin valve nano-stripes

Nicolas Rougemaille, Vojtech Uhlîr, Olivier Fruchart, Stefania Pizzini, Jan Vogel, Jean-Christophe Toussaint

# Phase diagram of magnetic domain walls in spin valve nano-stripes

N. Rougemaille,[1] V. Uhlíř,[2,1] O. Fruchart,[1] S. Pizzini,[1] J. Vogel,[1] and J. C. Toussaint[1,3]
[1)] *Institut NÉEL, CNRS & Université Joseph Fourier – BP166 – F-38042 Grenoble Cedex 9 – France*
[2)] *CEITEC BUT, Brno University of Technology, Technická 10, 61669 Brno, Czech Republic*
[3)] *Institut National Polytechnique de Grenoble – France*

(Dated: 26 February 2012)

We investigate numerically the transverse versus vortex phase diagram of head-to-head domain walls in Co/Cu/Py spin valve nanostripes (Py: Permalloy), in which the Co layer is mostly single domain while the Py layer hosts the domain wall. The range of stability of the transverse wall is shifted towards larger thickness compared to single Py layers, due to a magnetostatic screening effect between the two layers. An approached analytical scaling law is derived, which reproduces faithfully the phase diagram.

The fundamental study of magnetic domain walls (DWs) has found a playground in lithographically-defined nano-stripes. In the range of widths from a few tens to a few hundreds of nanometers their complexity is dramatically reduced with respect to extended thin films, while still retaining a few internal degrees of freedom leaving a rich physics. For stripes with in-plane magnetization head-to-head DWs are of transverse (TW) or vortex (VW) type (FIG. 1b)[1,2], and are characterized by a chirality, asymmetry and/or polarity. Their propagation under the stimulus of a magnetic field or a current of spin-polarized electrons is intrinsically precessional and revealed effects such as DW inertia[3] and a so-called Walker limit beyond which periodic DW transformations occur[4–7]. Due to their small size and fast dynamics, magnetic domain walls (DWs) are promising candidates in the area of information processing and storage[5,7].

Most reports so far have considered DWs in a single layer of magnetically-soft materials, such as Permalloy (Py) or CoFeB alloys. Magnetic trilayers F1/NM/F2 (with F$i$ a ferromagnet, and NM a non-magnetic material) also deserve attention as they play a key role in spintronics, for implementing Giant Magneto-Resistance (for a metal spacer, then called a spin-valve) and Tunneling Magneto-Resistance (for an insulator spacer, then called pseudo spin-valve or tunnel magnetic junction) devices. F1 is a soft layer in which the DW moves, while F2 is a reference layer that is supposed to remain uniformly magnetized. Unusually-large current-driven DW mobilities with speed exceeding 600 m/s have been reported in such stacks[8,9]. Tentative explanations point at either out-of-plane spin accumulation and torque[10,11], Oersted field[12] or magnetostatic coupling between the layers that may modify the statics or dynamics of the DW[12,13].

While the role of magnetostatic coupling is well established in thin films with the formation of quasi-walls in the supposedly uniformly-magnetized layer[14], it has scarcely been addressed[13] in stripes so far. In this Letter we determine the phase diagram of head-to-head DWs in spin valves with in-plane magnetization (TW versus VW), combining numerical simulation and analytical modeling. For this purpose, we consider Co/Cu/Py nanostripes with various widths $w$ and thickness of the individual layers $t_{\mathrm{Co}}$, $t_{\mathrm{Cu}}$ and $t_{\mathrm{Py}}$. The DW is located in the Py layer while the Co layer is initialized with uniform magnetization. We predict that the stability of TWs is enhanced towards larger Py thickness compared with single layers[1,2], due to the screening in the Co layer of the stray field arising from the DW in Py.

We used finite-differences micromagnetic codes, both OOMMF[15] and our home-made GL-FFT code[16]. The cell size in all simulations presented here is $4\times4\times5\,\mathrm{nm}^3$; differences with a smaller cell size $4\times4\times2.5\,\mathrm{nm}^3$ are minute. Effects of the finite length of the stripe in the simulations were reduced by either fixing the magnetic moments at both ends parallel to the stripe direction, or by compensating the surface magnetic charges at both ends however with no constraint on magnetization. The length $L$ of the stripes was set equal or larger than $20w$, for which finite-size effects are identically small under either of the above procedures. Material parameters are $\mu_0 M_{\mathrm{Co}} = 1.7593\,\mathrm{T}$, $A_{\mathrm{Co}} = 30\,\mathrm{pJ/m}$, $\mu_0 M_{\mathrm{Py}} = 1.0053\,\mathrm{T}$, $A_{\mathrm{Py}} = 10\,\mathrm{pJ/m}$, and zero magnetocrystalline anisotropy in both layers. No direct exchange coupling is considered. Different initial conditions were chosen in Py to set a TW or VW in the Py layer, while magnetization in Co is set uniform along the stripe direction; both layers are then set free to evolve during the simulation. We considered head-to-head DWs (two domains facing each-other, see FIG. 1a) with no loss of generality, as tail-to-tail DWs are equivalent under time-reversal symmetry ($\mathbf{M}\rightarrow-\mathbf{M}$). Like for single layers, TWs and VWs coexist as (meta)stable states in a large range of geometrical parameters. The iso-energy curve separating the areas where either a TW or a VW is lowest in energy, was determined for each fixed $w$ through a parabolic interpolation of the energy difference for three different values of $t_{\mathrm{Py}}$. We checked that this procedure yields a phase diagram of the single layer in very close agreement with existing reports[1,2].

We first discuss qualitatively the difference between a DW in a single layer and in a spin valve. The head-to-head DW in Py is associated with a total magnetic charge $+2t_{\mathrm{Py}}wM_{\mathrm{s}}$ (FIG. 1a). While VWs are similar in both systems, clear differences are found for TWs. In a single layer, TWs are symmetric for small thickness and width (FIG. 2). Going towards a larger thickness or width the TW becomes asymmetric, helping to re-

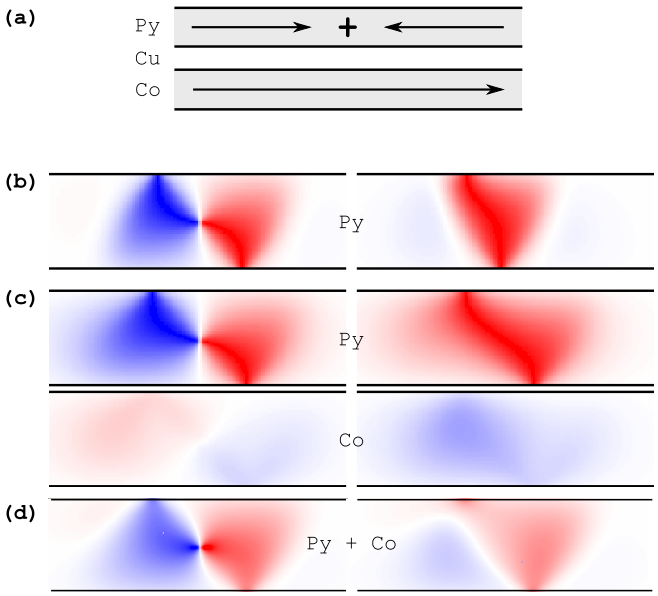


FIG. 1. (a) Cross-sectional sketch of a head-to-head domain wall and the associated charge in a spin valve. Plane views of a vortex wall and transverse wall in a 300 nm-wide (b) single layer of Py(5 nm) and (c) a Co(5 nm)/Cu(5 nm)/Py(5 nm) spin valve. (d) thickness-integrated maps of magnetization from (c), see Eq. (1). The red (blue) color indicates the positive (negative) transverse component of magnetization, normalized to the magnetization of the layer under focus in (b) and (b), and to half the magnetization of Co in (d).

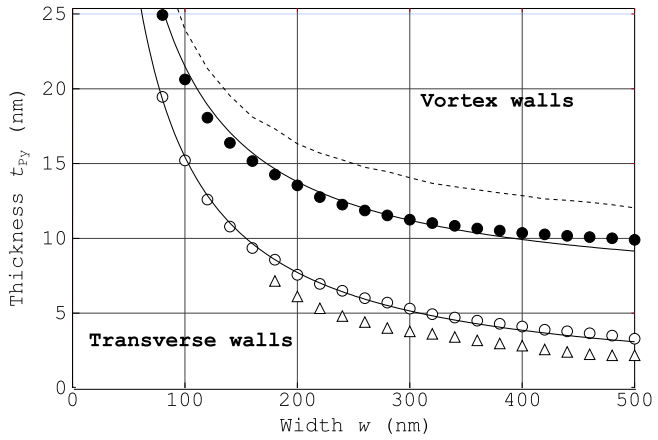


FIG. 2. Phase diagram of head-to-head domain walls in stripes, with the boundary between symmetric and asymmetric TWs (△) and TW and VW (○) in a single layer, and asymmetric TW and VW in a spin valve (•). From bottom to top, the three lines are: a $1/t_{\rm Py}$ fit to the TW-VW data for a single layer, a thickness translation of the former to fit the TW-VW data for a spin valve, and another thickness translation with $t_{\rm sh}(t_{\rm Cu}=0)$, see Eq. (3) and text.

duce magnetostatic energy by spreading the magnetic charges[2] (FIG. 1b); this corresponds to the onset of zigzag walls in continuous films. The transition from symmetric to asymmetric TW is of second order (continuous), so that for a given geometry only one type of TW may exist, either symmetric or asymmetric. Asymmetric TWs are found for a large range of values of width and thickness, although they are the state of lowest energy (over the VW) only in a narrow range of values (FIG. 2). In a spin valve the Co layer deviates from uniform magnetization due to the stray field arising from the DW in Py, which in turn creates a stray field influencing Py. This is a magnetic screening effect, which lowers the energy compared to a single layer, as already pointed out[13]. It is clear that the stray field arising from the DW in Py will be parallel or antiparallel to the initial direction of magnetization of Co, whether the left or right side of the DW (FIG. 1a) is considered. Thus the magnetic configuration of Co is expected to be asymmetric, and so will be the stray field arising from Co on Py. A TW in a spin valve is therefore expected to be always asymmetric by nature, due to the unidirectional magnetization in the Co layer.

FIG. 1c shows a VW and a TW in a spin valve, with the same width and Py thickness as in FIG. 1b. As expected the TW is asymmetric, to a greater extent than in the single layer case resulting in a larger DW width[13]; the magnetic screening in Co is clear from the non-uniformity of magnetization. Also both the VW and TW have a larger width and tails. Indeed, as a DW results from the balance of magnetostatic versus exchange energies, the decrease of magnetostatic energy allows to decrease exchange energy via the increase of the DW width. The flux closure taking place between Py and Co can also be illustrated by the map of magnetization integrated over the two layers along their normal (FIG. 1d):

$$\mathbf{M}_{\rm int} = \frac{1}{t_{\rm Co}+t_{\rm Py}} \int \mathbf{M}(z)\mathrm{d}z \qquad (1)$$

This map has some similarities with a VW, which highlights a clever way of reducing the total energy: the flux is better closed than in a single layer TW, while avoiding the cost associated with the vortex core in a single layer VW.

As the share of magnetostatic energy is larger in a TW than in a VW[1], the closure of flux mentioned above lowers the energy of the former more than that of the latter, suggesting that the TW is the ground state in a larger range of geometrical parameters in a spin valve than in a single layer. This is confirmed by a set of simulations with varying $t_{\rm Py}$ and $w$, illustrated in FIG. 2 for $t_{\rm Co} = t_{\rm Cu} = 5\,$nm. Notice that in a single layer TWs with opposite asymmetries (left or right) are degenerate in energy, while they are not in a spin valve, due to the unidirectional magnetization in the underlying Co. In the phase diagram (FIG. 2) we considered only the TW with the lowest energy.

We now derive a simple analytical model to grasp the main features of this diagram. McMichael and Donahue

already noticed that the iso-energy line in a single layer follows the power law $tw = C\Delta_d^2$ with $\Delta_d = \sqrt{A/K_d}$ the dipolar exchange length and $K_d = (1/2)\mu_0 M_s^2$ the dipolar constant. This law can be derived qualitatively by balancing the energies at play in each domain wall[1]. McMichael argued that the energy of the TW can be estimated from the lateral demagnetizing coefficient scaling like $t/w$ and the volume of the TW of the order of $tw^2$, while that of the VW is related to the energy of the vortex core for the VW, scaling with $t\Delta_d^2 K_d$. The exchange energy in the $\approx 90°$ Néel sub-walls can be ignored as the total length of these walls is identical in a TW and a VW. The numerical value $C \approx 61 - 64$ must be provided by simulations[1,2].

This scaling model can be adapted to a spin valve, however the above arguments must first be refined. It shall first be noted that in any head-to-head DW, either TW or VW, most of the energy is of magnetostatic origin and related to the head-to-head charges, so that the above argument is too naive. Simulation and magnetic force microscopy of a head-to-head DW in a single layer show that the total charge $Q = 2twM_s$ is nearly uniformly spread over the area of the DW[3], which is $\approx w^2$ for a TW, and $\approx 2w^2$ for a VW. The associated densities of surfaces charges are then $\sigma_{TW} = 2(t/w)M_s$ and $\sigma_{VW} = (t/w)M_s$. The resulting volume density of stray field energy scales with $\sigma^2$ and extends over a typical distance $w$ above and below the stripe. This results in an excess of magnetostatic energy in the TW over the VW of $\approx 2t^2 w K_d$. We now consider a spin valve. In the limit $t_{Py}M_{Py} > t_{Co}M_{Co}$, which is suitable for $t_{Co} = 5\,\text{nm}$ and the boundaries of the phase diagram of practical interest[1,2], the charges of the DW in Py are only partly screened, while the deformation in Co reaches its maximum. The above scaling laws can be rewritten accordingly and the following law is derived with some approximations, making also use of the partial flux closure in spin valves to refine the lateral demagnetizing coefficient[17]:

$$w(t - t_{sh}) \approx C\Delta_d^2. \tag{2}$$

This suggests that the phase diagram for a spin valve is based on that of a single layer, shifted towards higher thicknesses by a value $t_{sh}$. This is in very good agreement with the results of numerical simulation (FIG. 2). Quantitatively, the analytical formula for $t_{sh}$ is not simple, implying both power and logarithmic functions. However thanks to the slow variation of the latter, $t_{sh}$ can be approximated faithfully with $t_{Co}(M_{Co}/M_{Py}) \approx 1.75 t_{Co}$.

For $t_{Co} = t_{Cu} = 5\,\text{nm}$ the shift $t_{sh}$ determined from simulations is 5.4 nm, while the above analytical model predicts $1.75 t_{Co} \approx 8.75\,\text{nm}$. This difference hints at a partial screening from Co. This can be understood since in the scaling model we neglected the magnetostatic energy stored in the volume of the Cu spacer, locus of a magnetic field arising between the charges of opposite sign in Py and in Co. FIG. 3 shows $t_{sh}$ resulting

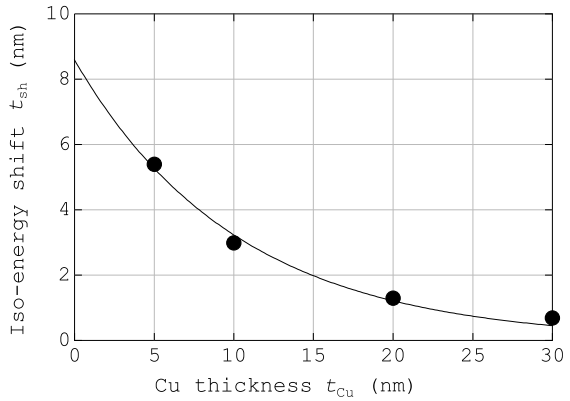


FIG. 3. Thickness shift of the iso-energy line in a spin-valve compared to a single layer, for stripe widths 100 nm (•), 300 nm and 500 nm.

from micromagnetic simulations as a function of $t_{Cu}$ for $w = 100\,\text{nm}$ and $t_{Co} = 5\,\text{nm}$. For large $t_{Cu}$ we tend towards the case of a single layer because the screening is no more effective. The decay is close to exponential, with a fit providing the extrapolation $t_{sh}(t_{Cu} = 0) \approx 8.60\,\text{nm}$. This figure is now in excellent agreement with the analytical model, which hints at the relevance of the following empirical law:

$$t_{sh} = t_{Co}\frac{M_{Co}}{M_{Py}} e^{-\frac{t_{Cu}}{t_0}}. \tag{3}$$

where $t_0 \approx 10\,\text{nm}$ is derived from FIG. 3. Further micromagnetic simulations show that $t_0$ increases with $w$, *e.g.* $t_0 = 13\,\text{nm}$ and 16 nm for $w = 300\,\text{nm}$ and 500 nm, respectively. This trend can be understood as the initial stray field (to be reduced) arising from the DW extends outside the stripe over a volume scaling with $w^3$, while the magnetic field arising between the charges of opposite sign in Py and in Co (a side cost of the screening effect) applies in a volume scaling with $t_{Cu}w^2$. Thus the relative gain of energy through screening decreases with decreasing stripe width. Having noticed this, Eq. (3) can be applied for other Co thicknesses, or more generally to other couples of magnetic materials if substituting the proper spontaneous magnetization values in Eq. (2), and fitting the decay of $t_{sh}$ like in FIG. 3.

One must finally keep in mind that for $t_{Py}M_{Py} < t_{Co}M_{Co}$ a very effective screening of the head-to-head DW charge is possible, so that deviations from Eq. (2) are expected. In that case the energy of the TW is drastically reduced. The iso-energy line becomes very flat beyond this limit, an effect that starts to be visible for the largest widths in FIG. 2.

To conclude we have investigated with numerical simulation and analytical scaling laws the phase diagram of head-to-head domain walls in F1/NM/F2 spin valves, with a domain wall in one layer and no domain wall in the other layer. We showed that the range of stability of

transverse against vortex walls is enhanced due to a magnetic screening effect. The iso-energy line in spin valves is translated towards a larger thickness with respect to single layers, by a value decreasing approximately exponentially with the spacer thickness. This enhanced stability and larger width provide a magnetostatic contribution to the enhanced mobility of DWs in trilayers, provided that the damping in Co is not too large[13]. Effects on the domain wall inertia and automotion[3] are also expected.


[1] R. McMichael and M. Donahue, IEEE Trans. Magn. **33**, 4167 (1997).

[2] Y. Nakatani, A. Thiaville, and J. Miltat, J. Magn. Magn. Mater. **290-291**, 750 (2005).

[3] J.-Y. Chauleau, R. Weil, A. Thiaville, and J. Miltat, Phys. Rev. B **82**, 214414 (2010).

[4] F. Cayssol, D. Ravelosona, C. Chappert, J. Ferré, and J. P. Jamet, Phys. Rev. Lett. **92**, 107202 (2004).

[5] D. A. Allwood, G. Xiong, C. C. Faulkner, D. Atkinson, D. Petit, and R. P. Cowburn, Science **309**, 1688 (2005).

[6] G. S. D. Beach, C. Nistor, C. Knuston, M. Tsoi, and J. L. Erskine, Nat. Mater. **4**, 741 (2005).

[7] S. S. P. Parkin, M. Hayashi, and L. Thomas, Science **320**, 190 (2008).

[8] J. Grollier, P. Boulenc, V. Cros, A. Hamzic, A. Vaurès, A. Fert, and G. Faini, Appl. Phys. Lett. **83**, 509 (2003).

[9] V. Uhlír, S. Pizzini, N. Rougemaille, J. Novotný, V. Cros, E. Jiménez, G. Faini, L. Heyne, F. Sirotti, C. Tieg, A. Bendounan, F. Maccherozzi, R. Belkhou, J. Grollier, A. Anane, and J. Vogel, Phys. Rev. B **81**, 224418 (2010).

[10] A. V. Khvalkovskiy, K. A. Zvezdin, Y. V. Gorbunov, V. Cros, J. Grollier, A. Fert, and A. K. Zvezdin, Phys. Rev. Lett. **102**, 067206 (2009).

[11] C. T. Boone, J. A. Katine, M. Carey, J. R. Childress, X. Cheng, and I. N. Krivorotov, Phys. Rev. Lett. **104**, 097203 (2010).

[12] V. Uhlir, S. Pizzini, N. Rougemaille, V. Cros, E. Jimenez, L. Ranno, O. Fruchart, M. Urbanek, G. Gaudin, J. Camarero, C. Tieg, F. Sirotti, E. Wagner, and J. Vogel, Phys. Rev. B (2011), in press.

[13] J. M. B. Ndjaka, A. Thiaville, and J. Miltat, J. Appl. Phys. **105**, 023905 (2009).

[14] J. Vogel, S. Cherifi, S. Pizzini, F. Romanens, J. Camarero, F. Petroff, S. Heun, and A. Locatelli, J. Phys.: Condens. Matter **19**, 476204 (2007).

[15] "http://math.nist.gov/oommf/," .

[16] O. Fruchart, J. C. Toussaint, P. O. Jubert, W. Wernsdorfer, R. Hertel, J. Kirschner, and D. Mailly, Phys. Rev. B **70**, 172409 (2004), brief Report.

[17] O. Fruchart and B. Diény, J. Magn. Magn. Mater. **324**, 365 (2011).


## ACKNOWLEDGEMENTS

This work was partially supported by ANR-07-NANO-034 *Dynawall* and ANR-08-BLAN-0199 *MicroManip*. VU was supported by the research programmes of GAAV (Project No. KAN400100701) and European Regional Development Fund (CEITEC - CZ.1.05/1.1.00/02.0068).